Int. J. Multiphase Flow Vol. 13, No. 3, pp. 403–413, 1987
Printed in Great Britain.

0301-9322/87 $3.00 + 0.00

AXISYMMETRIC SURFACE-TENSION-DRIVEN FLOW

K. V. DAPKUS and P. J. SIDES†
Department of Chemical Engineering, Carnegie-Mellon University, Pittsburgh, PA 15213, U.S.A.

(*Received* 20 *August* 1985; *in revised form* 19 *September* 1986)

Abstract—In studies of electrolytic gas evolution at an ideally smooth surface, a non-uniform double-layer potential on a mercury pool in contact with aqueous sulfuric acid, corresponding to a non-uniform electrolytic current distribution at the interface, established a varying surface-tension distribution that drove flow of both solution and mercury phases. Interfacial flow velocities were measured by photographing the nucleating bubbles as they were transported to the periphery of the pool. Compared were theoretical and experimentally determined velocity profiles of this axisymmetric surface-tension-driven flow.

INTRODUCTION

Experimenting with nucleation of hydrogen gas bubbles, we electrolytically evolved hydrogen gas at a mercury cathode from sulfuric acid solution (Dapkus 1985; Dapkus & Sides 1986). The hydrogen molecules diffused away from the mercury electrode to the well-mixed region in the bulk because of the concentration gradient present, but they could not diffuse away fast enough to prevent local supersaturation of the electrolyte because hydrogen is sparingly soluble in sulfuric acid. When the dissolved hydrogen gas concentration reached a critical value, bubbles nucleated and began growing. A feature of this experiment was an axisymmetric surface-tension-driven flow that continuously freshened the mercury at the axis of the cell. Knowing the magnitude of the velocities of that flow was important to the experiment because the flow established the convective–diffusion conditions that determined the rate of hydrogen transport from the electrode. Discussed in the following is the agreement between theory derived for this flow and experimental data on the flow velocities.

Figure 1 is a schematic of the electrolytic cell that consisted of an anode chamber containing a platinum anode suspended over a cathode chamber containing a mercury pool. Connecting the two chambers was a glass tube that directed the electric current toward the center of the pool. The non-uniform current distribution at the mercury surface engendered a radially varying interfacial double-layer potential greatest at the center of the mercury pool where the current density was the highest (Dapkus & Sides 1986). The double-layer potential decreased as a function of radius from the center to the periphery of the pool, and the interfacial surface tension therefore increased correspondingly, as governed by the Lippmann equation (Newman 1973); hence the lower surface tension are at the center of the mercury pool flowed outward to relieve the high surface-tension area at the periphery. Both the mercury phase and the aqueous phase were thus continuously pumped outward at the interface by the steady-state variation of the interfacial potential. The radial flow of the interface meant that fresh mercury appeared continuously at the center of the pool, where the probability of bubble nucleation was the highest; interfering matter was swept out of the critical region.

The velocity profiles are sketched qualitatively in figure 2. Since the interface flowed radially outward, solution from outside the glass tube replenished the electrolyte at the center of the mercury pool. We observed this reversal in the velocity experimentally when a hydrogen bubble in the electrolyte phase was swept out with the interface and returned by the recirculating flow.

The Navier–Stokes equations describing the flow in both phases near the axis and interface separate when assumptions analogous to the von Karman substitutions for the rotating disk are used (Sides 1982). The boundary condition at the mercury–electrolyte interface separates only when the interfacial tension varies as the square of the radius. The surface is uniformly accessible from both phases only when this artificial condition is met. In principle the solution is valid only when

†To whom all correspondence should be addressed.

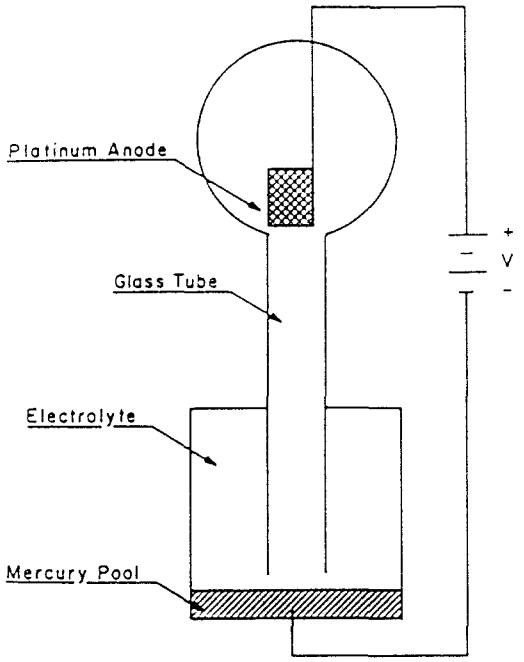

Figure 1. Simplified schematic of the mercury pool cell.

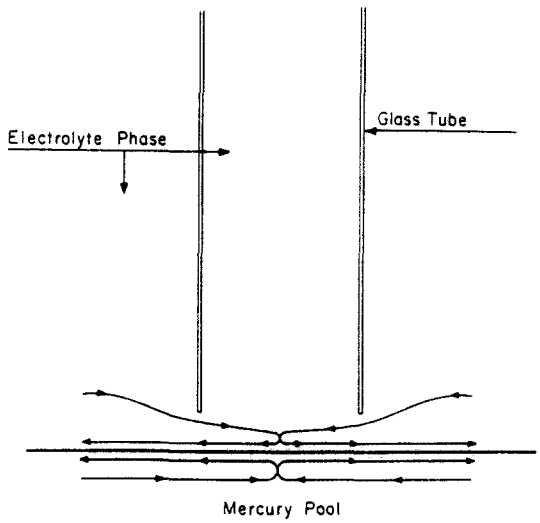

Figure 2. Qualitative sketch of the velocity field.

the electrolytic cell is designed to create a radial surface tension distribution proportional to the square of the radius; in practice the existing variation of interfacial tension was approximated as a parabola. In this contribution, we show how the predictions made by means of this approximation agreed with experimentally obtained velocities.

EXPERIMENT

The apparatus for the experiment is shown in figure 3. The main vessels were the bubbler, the pre-electrolyzer and the cell itself. Sulfuric acid was poured into the bubbler and then sparged with purified hydrogen for 48 h to eliminate dissolved oxygen that would have oxidized the mercury surface. Pure hydrogen has no affect on the surface tension of mercury as compared with the value *in vacuo* (Wilkinson 1972); likewise, pure hydrogen has no effect on the mercury–water interfacial surface tension. After purging, the hydrogen-saturated solution the flowed into the pre-electrolyzer, previously charged with mercury, and was pre-electrolyzed for 72 h, which removed base-metal impurities present in the electrolytic solution. After 72 h of pre-electrolysis, the electrolyte flowed into the cell and contacted the mercury previously charged to the cathode compartment. Carefully purified aqueous solutions of 0.1 N, 1 N and 96 wt% sulfuric acid were used.

A detailed cell diagram is given in figure 4. The large window in the front center allowed observation of the mercury–solution interface from an angle of about 60° above the horizontal. The two smaller 25.4 mm windows were used for illumination during filming of the nucleation event. Light introduced through a side window reflected off the interface and shone out the other side window unless a bubble caught it; hence a dark-field image of the bubble was obtained. The cell also featured a port for the reference calomel electrode that was used for measuring the potential at nucleation.

Constant current was applied to the cell by a Princeton Applied Research Model 173 galvanostat. The flow of the interface was recorded on reversal film using a 16 mm Bolex camera and an American Optical model 55M-2 microscope, at a magnification of 10×. The potential of the mercury pool corresponding to the current passing through the cell was recorded on a Nicolet oscilloscope.

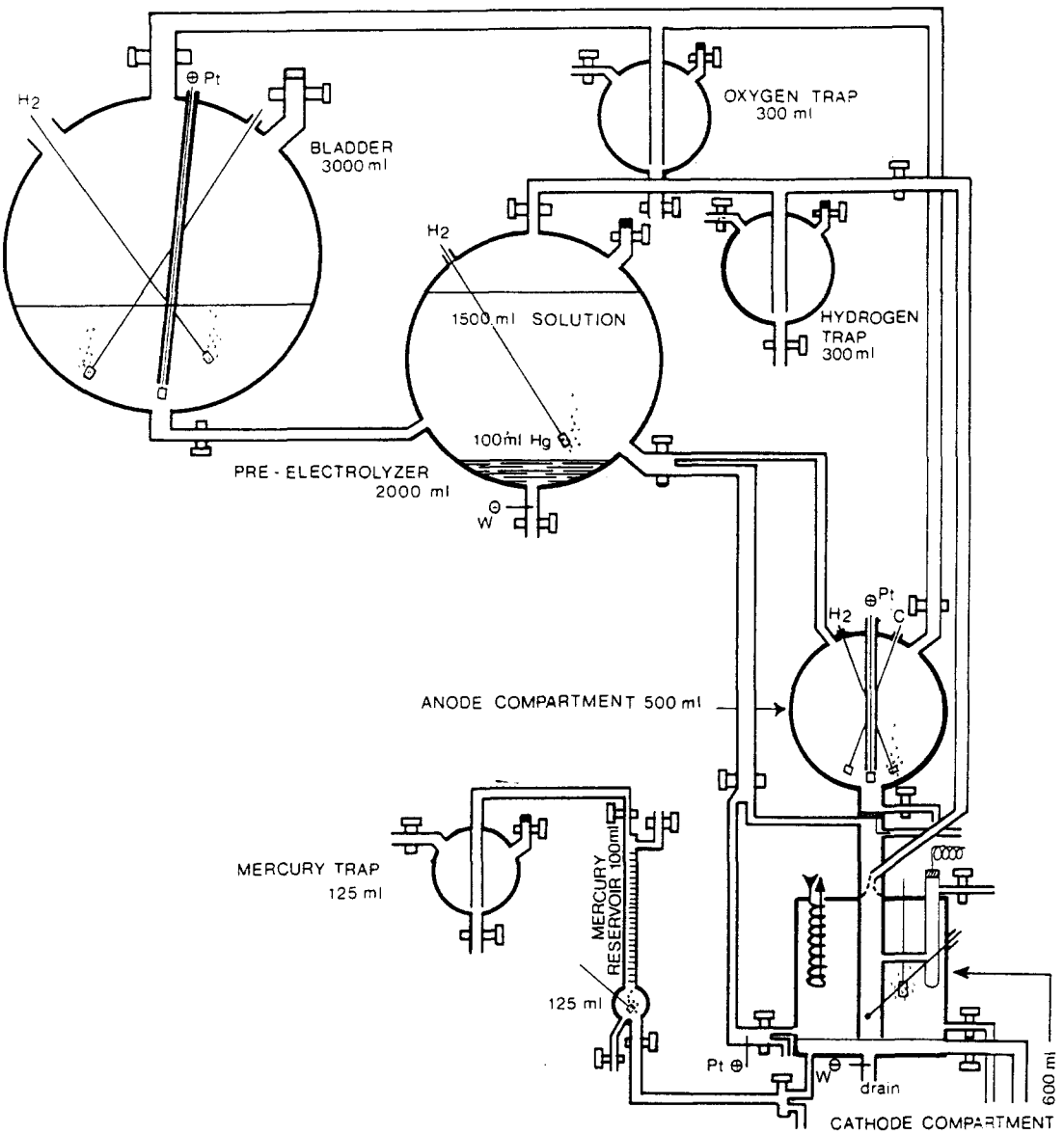

Figure 3. Experimental apparatus.

RESULTS

At low potentials, the mercury was motionless, but as the potential was increased, the surface of the mercury pool began to move and mercury was "pumped" from below to replace it. The radial velocity was greatest at the mercury–electrolyte interface. The center of the mercury pool, where nucleation occurred, was continuously renewed.

A sequence of frames from the films is shown in figure 5. The dark-field photographs each show the bright arc that is the reflection of the curved rim of the central glass tube. The frame corresponds to 25.4 actual mm. In the first of the 4-frame sequence, only a few bubbles attached to the glass tube appear; the black area in the center is the mercury surface. In the second frame, a bubble indicated by the arrow appears near the center of the photograph and then translates radially as shown in the succeeding frames. In the final frame the bubble is elongated because its velocity at this point is comparable to the framing rate of the camera.

We measured the radial velocity of the interface by determining the velocity at which the gas bubbles translated radially outward to the periphery. The bubbles cannot travel faster than the

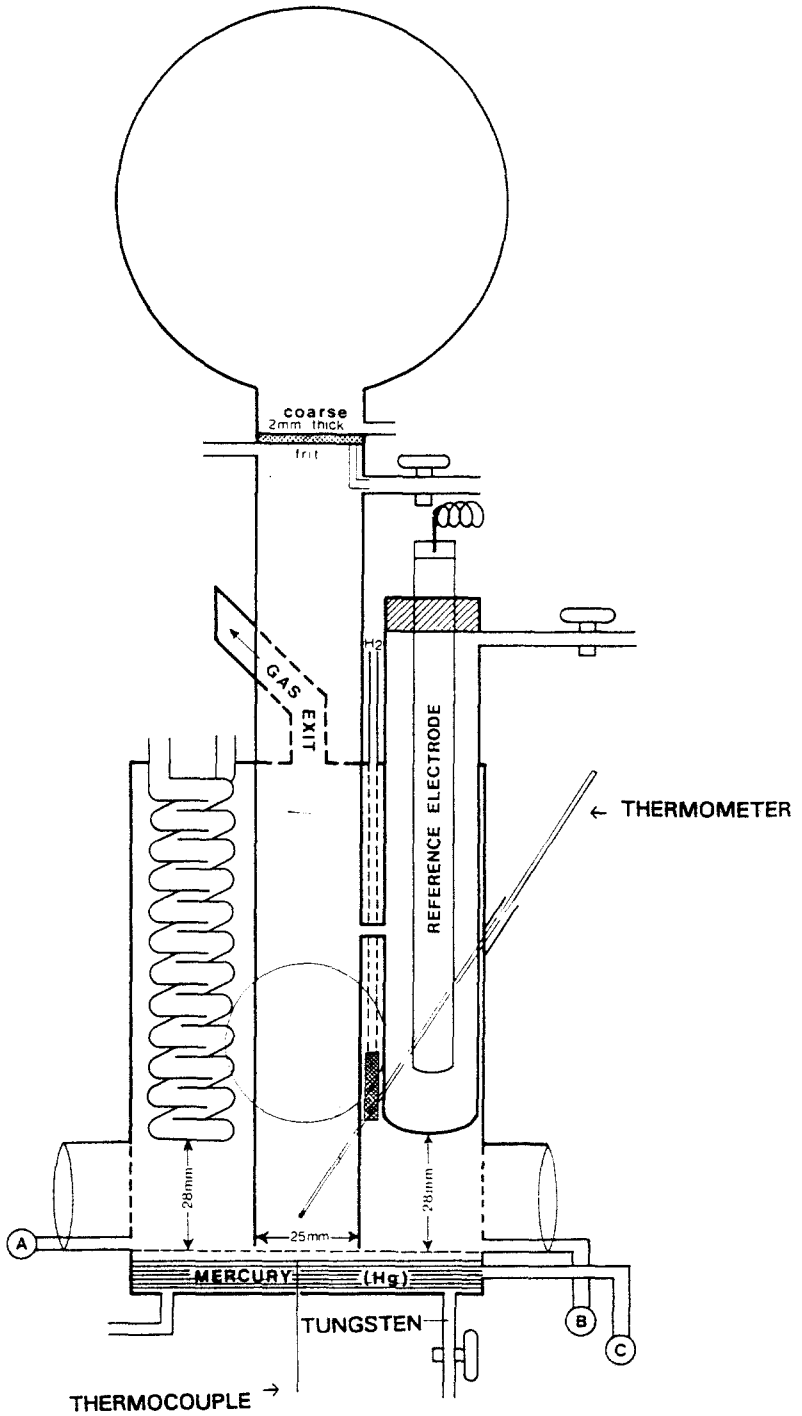

Figure 4. Electrolytic cell.

interface, hence their velocity must be a minimum velocity of the interface. The bubbles appeared to travel with the interface in most cases. The experimentally obtained bubble velocities, in mm/s, plotted as a function of the radial position along the mercury surface, in mm, are shown in figure 6 for the 1.0 N H_2SO_4 and 0.1 N H_2SO_4 electrolytes. The axis of the mercury pool corresponds to $r = 0$ and $r = 12.55$ mm corresponds to the outside radius of the center glass tube. Only that portion of the mercury pool lying directly below the center glass tube was important. As previously noted, this area is only about 25.4 mm dia. The lines marked by $a = 53$ N/m^3 and $a = 40$ N/m^3 will

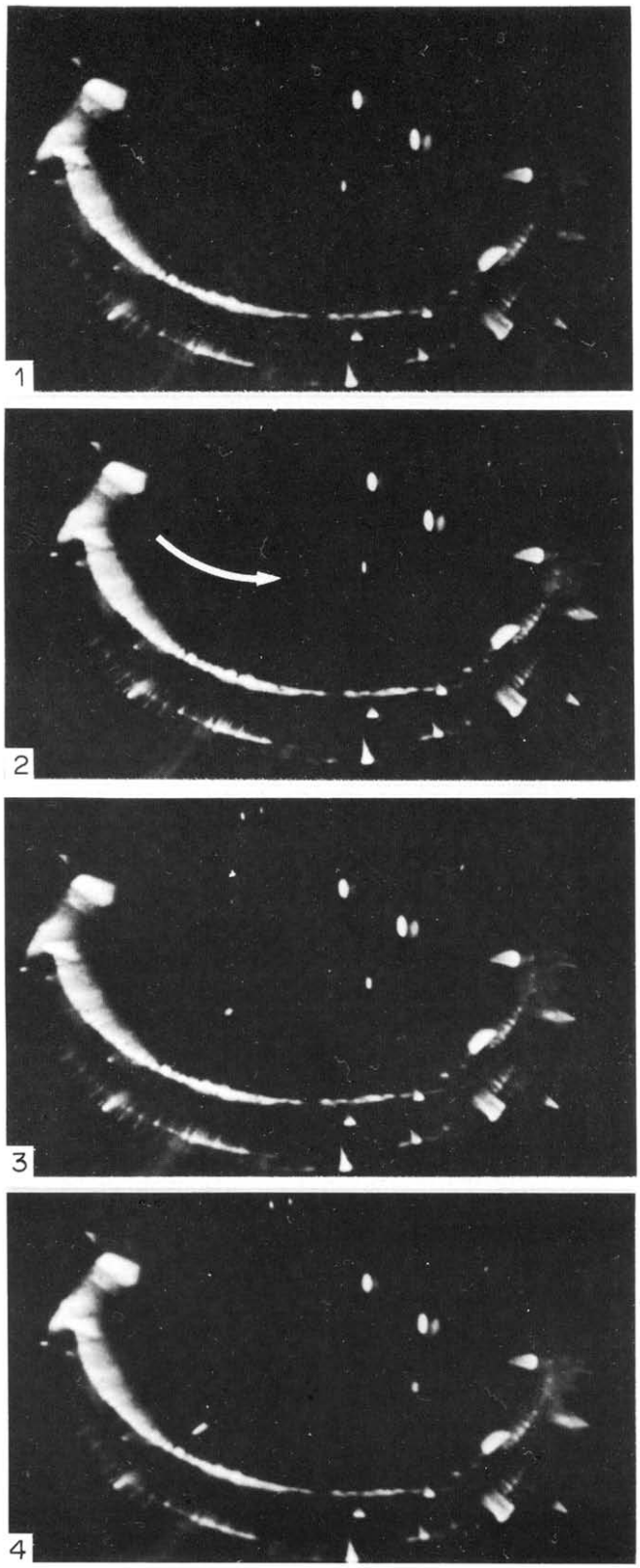

Figure 5. Radial bubble motion from the film: (1) no bubble present; (2) bubble appears faintly at the arrow; (3) bubble travels radially outward; (4) elongated image of bubble means its velocity is fast with respect to the framing rate of the camera.

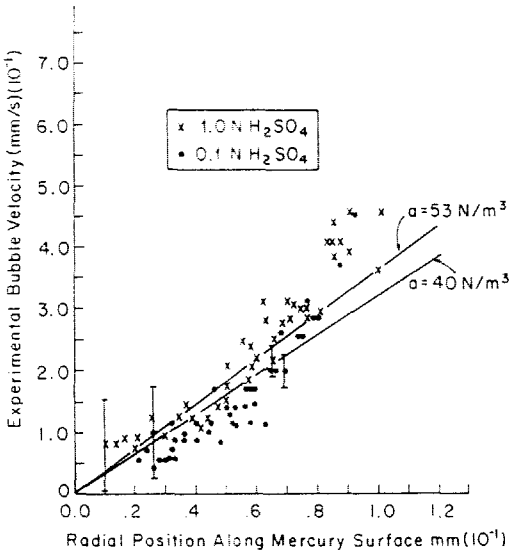

Figure 6. Experimental bubble velocities for 1.0 and 0.1 N H_2SO_4.

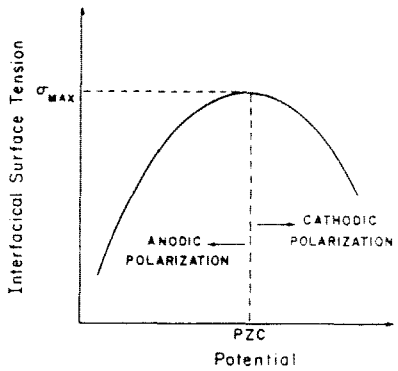

Figure 7. Qualitative sketch of the electrocapillary curve.

be discussed later. The scatter in the velocity data is due to measurement error especially at the center where the velocities are the lowest. Note that the experimental velocities for the 0.1 N H_2SO_4 electrolyte are slightly lower than for the 1.0 N H_2SO_4 case.

An additional experiment, in which nearly pure sulfuric acid (95 wt%) was the electrolyte, was also performed. In this case the fluid flow was reversed, with the center being the focus of the flow that came in from the periphery.

DISCUSSION

The electrocapillary curve for the mercury–sulfuric acid interface, qualitatively sketched in figure 7, governs the dynamic behavior of the two fluids. The slope of the electrocapillary curve is proportional to the electric charge density on the mercury surface; hence the maximum in the electrocapillary curve is the point of zero charge (PZC) that occurs, for 1.0 N H_2SO_4 at 25°C, at approx. −27 V, and corresponds to a maximum surface tension of 0.423 N/m (Jofa *et al.* 1939). When the potential within the double layer is different from the PZC, the mercury is polarized. During our experiments, the mercury pool was always negatively polarized, i.e. toward the r.h.s. of figure 7. Therefore, the center of the mercury pool, where the current density and hence the polarization was the highest, had the lowest interfacial surface tension and the periphery had the highest interfacial surface tension.

The experiment with 95 wt% sulfuric acid was an exception to this because the electrocapillary curve had shifted. A side reaction, most likely the reduction of sulfate to sulfurous acid and thence to hydrogen sulfide, occurred in a potential range such that the surface tension at the periphery was less than the tension at the center. Mindyuk & Gutman (1965) has discussed the effect of increasing sulfuric acid concentration on the electrocapillary curve. As the concentration increases, the point of zero charge shifts to more cathodic potentials. For such a high concentration of sulfuric acid, the maximum in the surface tension has shifted far enough so that the radially increasing potential corresponds to a decrease in interfacial tension; hence the interface flows toward the axis.

Current, potential and interfacial surface-tension distribution

To compare the theoretical predictions with the experimentally obtained flows, we solved Laplace's equation in the electrolyte (Newman 1973) for the potential distribution on the electrode surface, and hence obtained the corresponding interfacial tension variation. The boundary-value problem was

$$\nabla^2\Phi = 0, \quad [1]$$

where

$$\nabla\Phi = 0 \quad [2]$$

at the pool's axis and on all glass surfaces, and

$$\Phi = 0 \quad [3]$$

at the position of the reference electrode in the center tube. The kinetic limitations of the hydrogen reaction on the mercury surface were represented by the Tafel equation, a rate expression for an electrochemical reaction, that related the electrode potential to the electric field at the interface:

$$V - \Phi_0 = \mathrm{a} + \mathrm{b}\log(-\kappa\nabla\Phi)_{\text{interface}}, \quad [4]$$

where

V = potential of mercury pool with respect to a hydrogen reference electrode,
Φ_0 = potential in solution outside the double layer,
a = experimentally determined constant,
b = experimentally determined constant

and

κ = conductivity.

Numerous studies of hydrogen overvoltage on a mercury surface have indicated that the Tafel equation is valid in the current-density ranges of 10^{-5}–1 A/m^2 (Frumkin 1943; Jofa *et al.* 1939). For 1.0 N H_2SO_4 the Tafel constants (a, b) are (−1.44, −0.116) and for 0.1 N H_2SO_4 they are (−1.43, −0.113).

We chose the finite-element method for solving the problem because of the complex geometry of our electrolytic cell, and the non-linear boundary conditions. Consider the system geometry appearing in figure 8. Only the lower 76 mm of the center glass tube is included in the solution domain. The potentials at the top three horizontal nodes are at the zero of potential and correspond to the position of the calomel reference electrode. As shown in figure 8, the solution region was divided into seven distinct regions called blocks consisting of equal-size triangular elements. Whenever possible, equilateral triangles were used to improve on the computational accuracy. The total number of nodes was 165, while the individual elements totaled 249. Because of axial symmetry, the solution region was reduced by half. In figure 8 there are only 16 nodes along the mercury surface and no nodes are positioned within the small gap between the center glass tube and the mercury surface where the potential varies significantly. To increase the accuracy of the resulting current-density distribution, the last row of elements along the mercury surface was subdivided twice to increase the number of nodes along the mercury surface in figure 8 to 61. The total number of nodes increased to 302, and the number of elements to 474. In addition, the number of nodes within the small gap increased to 7. Details of the solution can be found elsewhere (Dapkus 1985).

A summary of the electrical and interfacial phenomena appears in figure 9. A similar diagram was generated for the 0.1 N case. The calculated current density is a maximum at the center and drops rapidly outside the central tube. The non-uniformity in the secondary current-density distribution corresponds to a radially varying double-layer potential and hence to the variation of the interfacial tension. The surface-tension functionality was obtained from the surface over-potential data and the corresponding electrocapillary curves.

Analysis of the flow and comparison with data

The mercury surface near the axis of the pool in this geometry is uniformly accessible if the interfacial surface tension varies as the square of the radius. The general form is given by the following equation:

$$\sigma = \frac{\alpha r^2}{2} + \beta, \quad [5]$$

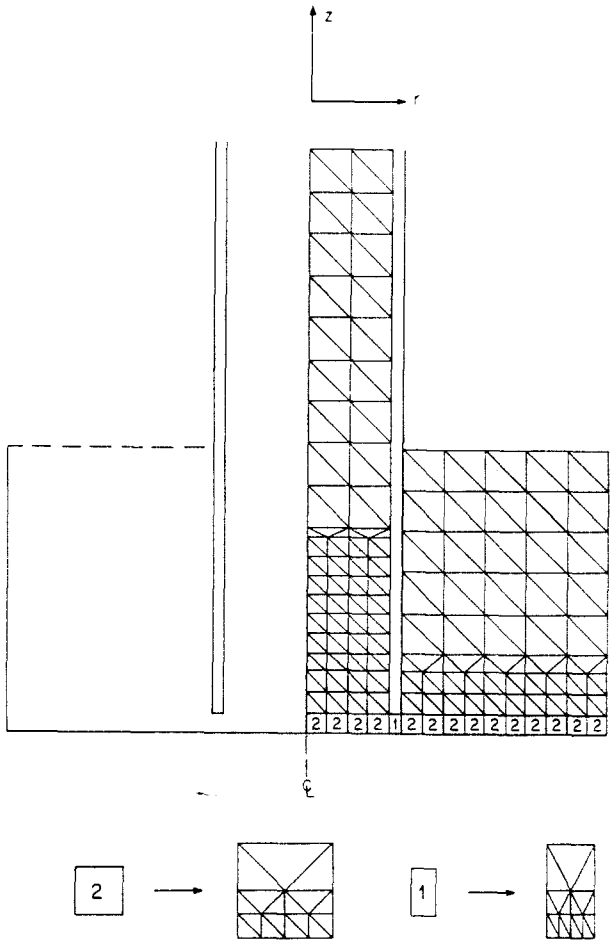

Figure 8. Finite-element model for the electrolytic cell.

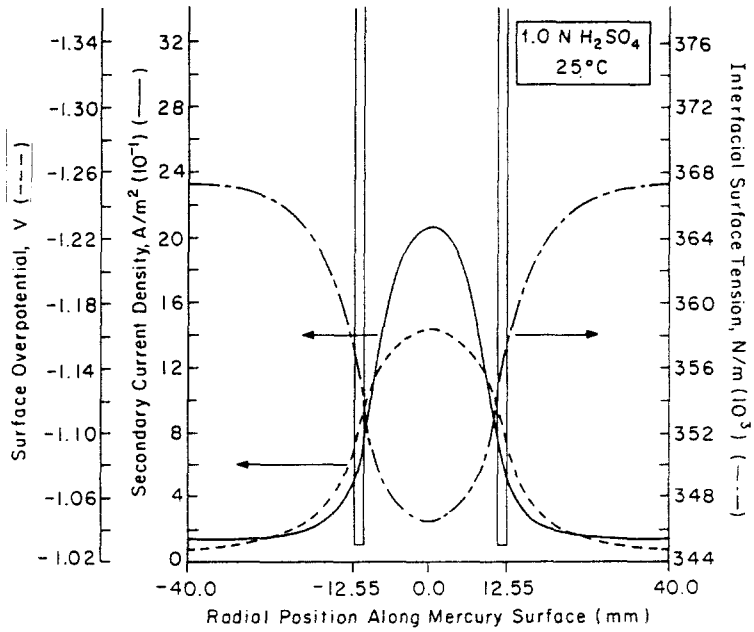

Figure 9. Effect of non-uniform current distribution on surface overpotential and interfacial tension for 1.0 N H_2SO_4.

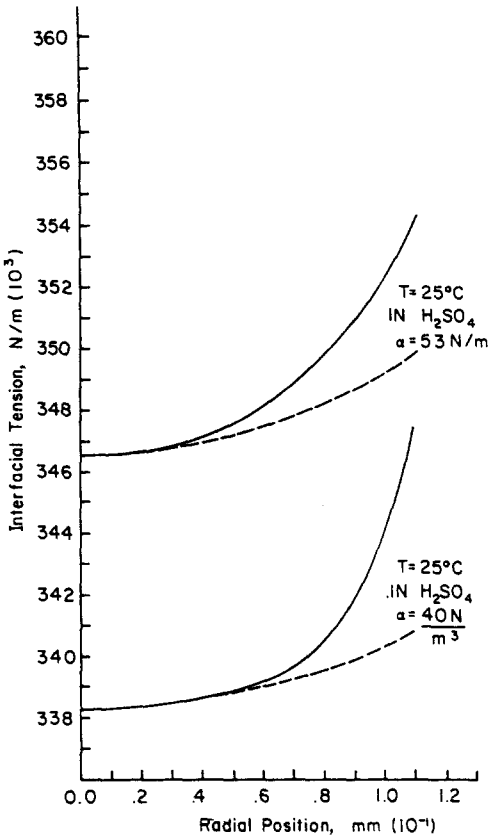

Figure 10. Surface-tension functionality curves for 1.0 and 0.1 N H_2SO_4.

where α, β are constants to be determined and σ has units of N/m. This restriction on the surface tension functionality is not satisfied exactly for an arbitrary system geometry and for all current densities; nevertheless, where the surface-tension variation can be fitted with a parabola, one might expect the flow to follow the theoretical results. To test the agreement between the calculated and the experimentally determined velocities, interfacial tension values for 1 N H_2SO_4 as well as for 0.1 N H_2SO_4 were plotted as a function of radial position in figure 10. Plotted in the same figure is the best-fit to the surface-tension functionality near the center of the mercury pool for these two cases. The parameters (α, β) for this best-fit curve near the pool axis are (53, 0.347) for 1.0 N H_2SO_4 and (40, 0.338) for 0.1 N H_2SO_4. The parabolas fit the calculated surface tension from the axis to a radial position of about 4 mm. The center of the mercury pool was the area most critical to the analysis.

The theoretical radial velocity of the interface is given by the following expression (Sides 1982), that is a consequence of the assumptions made to separate the Navier–Stokes equations:

$$V_r = f_0 Fr, \qquad [6]$$

where

V_r = the radial velocity of the interface,
f_0 = the dimensionless parameter defined as $\alpha z_0/\mu$,
z_0 = dimensionless parameter defined as $(\mu^2/\rho\alpha)^{1/3}$,
F = dimensionless radial velocity, a function of axial distance only,
μ = viscosity of the aqueous phase

and

ρ = density of the aqueous phase.

At the interface, the value of F is 0.27 as taken from the theoretical calculation (Sides 1982, figure 2). Likewise, using the value for "α" of 53 N/m^3 for 1.0 N H_2SO_4 and 40 N/m^3 for 0.1 N H_2SO_4, f_0 is calculated to be 13.58 and 11.88 s, respectively for the aqueous phase. The corresponding expressions for the radial velocity for 1.0 N H_2SO_4 and 0.1 N H_2SO_4 become

$$V_r = 3.66\, r/s \qquad [7]$$

and

$$V_r = 3.21\, r/s \qquad [8]$$

where r is the radial distance from the axis in mm. The radial velocity of the interface for both electrolytes should be linear with radius.

Equations [7] and [8] appear along with the experimentally determined bubble velocities in figure 6. The comparison is valid because the slopes of the radial velocity profile in [7] and [8] depend only on the value for "α", the interfacial surface-tension constant obtained from the calculated secondary current-density distribution, and the hydrodynamic solution (Sides 1982). The value of the slope is independent of the bubble velocities obtained from the experiment.

The experiment bubble velocities are roughly linear with distance from the pool axis up to a distance of 6 mm, which is consistent with these equations. The agreement between the equations and our experimental results is reasonable in magnitude, but scatter in the data, especially near the axis, prevented more precise assessment of the degree of linearity near the center. As predicted by the theory, the velocities obtained in the 1.0 N case exceeded the velocities in the 0.1 N solution. These results were nevertheless sufficient to carry out the necessary calculations for the main experiment.

One expects the linearity to break down between 4 and 8 mm from the axis because, from figure 10, the surface-tension function does not match the calculated one beyond this distance. The bubbles should move faster than predicted at the periphery because the interfacial tension is changing more rapidly with distance. Indeed the experimental data demonstrate that the more rapidly changing interfacial tension near the glass tube at 12.5 mm from the axis accelerates the bubbles and the deviation from the rough linearity is obvious.

The theoretical velocities exceed the experimental velocities in the region between 0 and 6 mm from the axis (with the exception of the least accurate points at the axis in the 1.0 N case) because the bubbles were travelling at a velocity equal to or less than the velocity of the interface. The bubbles cannot travel faster than the interface; in fact, their velocity should be somewhat less than the velocity because drag must act on them. The results from the experiment exceeded the theoretical predictions beyond 8 mm from the axis because the double-layer potential, and hence the interfacial tension, changed most rapidly with radius near the glass tube.

CONCLUSIONS

A mercury pool cell was used to study the nucleation of electrolytically evolved gases. A non-uniform electrolytic current distribution corresponding to a non-uniform double-layer potential, and hence a non-uniform surface-tension distribution, drove an interfacial flow which continuously renewed the critical area of the experiment. As part of that experiment, interfacial velocities of a surface-tension-driven flow were measured. Reasonable agreement between theoretical and experimentally determined velocity profiles of an axisymmetric surface-tension-driven flow was obtained.

Acknowledgement—This work was supported by the National Science Foundation.

REFERENCES

DAPKUS, K. V. 1985 Nucleation of electrolytically evolved gases at an ideal electrode. Ph.D. Thesis, Carnegie–Mellon Univ., Pittsburgh, Pa.

DAPKUS, K. V. & SIDES, P. 1986 Nucleation of electrolytically evolved hydrogen at an ideally smooth electrode. *J. Colloid Interface Sci.* **111**, 133–151.

FRUMKIN, A. 1943 Contribution to the theory of the discharge of hydrogen ions. *Acta phys.-chim. URSS* **18,** 23.

JOFA, S., KABANOV, E., KUCHINSKI, E. & CHISTYAKOV, F. 1939 Overvoltage on mercury in the presence of surface active electrolytes. *Acta phys.-chim. URSS* **10,** 317.

MINDYUK, A. K. & GUTMAN, E. M. 1965 Surface activity of some acid corrosion inhibitors. *Fizika Khim. Mekh. Mater.* **1,** 626.

NEWMAN, J. 1973 *Electrochemical Systems.* Prentice-Hall, New York.

SIDES, P. 1982 Axisymmetric flow driven by a surface tension gradient at a mobile interface. *Int. J. Multiphase Flow* **8,** 553–558.

WILKINSON, M. C. 1972 The surface properties of mercury. *Chem. Rev.* **72,** 575.